

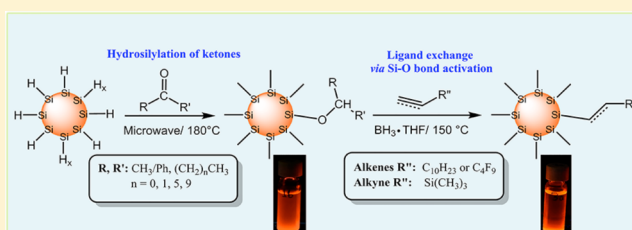
Alkoxy-Terminated Si Surfaces: A New Reactive Platform for the Functionalization and Derivatization of Silicon Quantum Dots

Tapas K. Purkait,* Muhammad Iqbal,[†] Muhammad Amirul Islam, Md Hosnay Mobarok, Christina M. Gonzalez, Lida Hadidi, and Jonathan G. C. Veinot*

Department of Chemistry, University of Alberta, Edmonton, Alberta T6G 2G2, Canada

S Supporting Information

ABSTRACT: Alkoxy-terminated silicon quantum dots (SiQDs) were synthesized via hydrosilylation of aliphatic ketones on hydride-terminated SiQD (H-SiQD) surfaces under microwave-irradiation. Aromatic ketones undergo hydrosilylation on H-SiQD surfaces at room temperature without requiring any catalyst. The alkoxy-terminated SiQDs are soluble in organic solvents, colloidal stable, and show bright and size dependent photoluminescence (PL). The alkoxy-functionalized silicon surfaces were used as reactive platform for further functionalization via unprecedented ligand exchange of the alkoxy-surface groups with alkyl or alkenyl-surface groups in the presence of $\text{BH}_3 \cdot \text{THF}$. Proton nuclear magnetic resonance (^1H NMR), Fourier transform infrared (FTIR), and X-ray photoelectron spectroscopy (XPS) spectroscopy confirmed alkoxy-terminated surfaces and their ligand exchange reactions in the presence of various alkenes and alkynes.



INTRODUCTION

Silicon is the second most abundant element in the earth's crust; it is also the semiconductor on which the electronics industry is built. As is the case for most semiconductors, silicon exhibits intriguing size-dependent properties when prepared on the nanoscale that have facilitated the development of prototype applications in many areas including electronics,¹ photonics,² photovoltaics,^{3,4} and catalysis.⁵ In addition to particle size, surface chemistry offers another degree of freedom that provides tailoring of silicon quantum dot (SiQD) properties.^{6–8} SiQDs have also garnered attention because of the promise of low cytotoxicity, which makes them well-suited as theranostic materials.^{9–11} If the full practical potential of SiQDs is to be realized they must be effectively interfaced with their surroundings (e.g., solubility) and rendered resistant toward deleterious and unwanted reactions (e.g., oxidation).⁶ To this end, establishing convenient methods for passivating and derivatizing SiQD surfaces to obtain functional (even “designer”) materials for practical or relevant industrial applications is of paramount importance.

To date, hydrosilylation reactions have been by far the most common basis for SiQD surface modification.^{12–16} These procedures see surface Si–H bonds on air-sensitive, insoluble hydride terminated SiQDs (H-SiQDs) added across carbon–carbon multiple bonds to yield robust Si–C surface linkages. Despite their appeal and versatility, these hydrosilylation approaches and the materials they provide can suffer from important limitations including size-dependent reactivity,¹⁷ ill-defined surface species,^{18,19} toxic metal-based impurities,²⁰ and limited surface coverage.^{17,19}

Furthermore, while the robust Si–C bond imparts material stability and solvent compatibility, it also limits further surface modification via ligand exchange protocols that are commonly employed with other nanoparticles.^{21,22}

Reaching beyond hydrosilylation, SiQD surfaces have been functionalized by attaching moieties through Si–N,^{8,23} Si–S,²² and Si–O bonds.^{24,25} Among these, Si–S bonds are particularly reactive.²⁶ Korgel et al. prepared alkanethiol-functionalized SiQDs and demonstrated subsequent ligand exchange with long chain alkenes;²² the lability of the Si–S bond presumably played a key role in these exchange reactions. While having reactive surface groups is advantageous for further surface modification, they can potentially leave the QD surface susceptible to unwanted reactions (e.g., oxidation and hydrolysis).

Alkoxy-terminated SiQDs (RO-SiQDs) bearing surface groups tethered through Si–O bonds have been prepared upon reaction of halide-terminated SiQDs with alcohols.^{24,25} Similar surfaces were also obtained on bulk hydride terminated Si(111) through thermally/photochemically induced functionalization with alcohol and aldehydes.^{27–30} It was also shown that an aldehyde group is almost unreactive toward H-terminated Si surfaces than an alkene group when both functionality present.³¹ The molecular hydrosilylation reaction of aldehydes and ketones is well-established and electron rich aromatic ketones undergo hydrosilylation with molecular silanes in the presence of Lewis acid catalysts.^{32,33}

Received: March 26, 2016

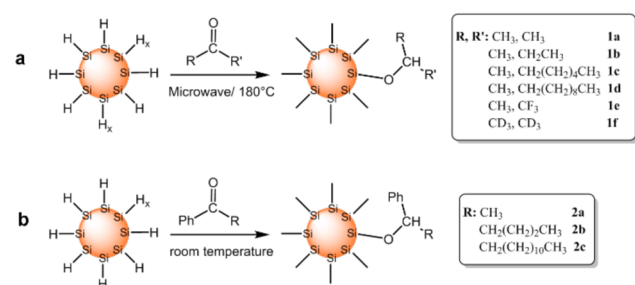
Published: May 19, 2016

To our knowledge the analogous reaction with carbonyl compounds has not been reported or fully exploited for H-SiQDs. Herein, we report the hydrosilylation of aliphatic and aromatic ketones by H-SiQDs. We also demonstrate that these alkoxy-terminated SiQDs provide a versatile solution processable reactive platform for further surface modification via unprecedented ligand exchange reactions with alkenes/alkynes in the presence of $\text{BH}_3\cdot\text{THF}$.

RESULTS AND DISCUSSION

Alkoxy-Terminated SiQDs. To access and exploit the reactivity of alkoxy-terminated SiQDs it was necessary to prepare H-SiQDs using well-established procedures developed in the Veinot Laboratory.^{16,34} SiQDs of three average diameters (i.e., $d \sim 3, 5, 8$ nm; vide infra)³⁵ were investigated and were modified with alkoxy-surfaces by exploiting hydrosilylation reactions (Scheme 1a). This procedure yielded transparent

Scheme 1. Synthesis of Alkoxy-Terminated SiQDs via Hydrosilylation of (a) Aliphatic and (b) Aromatic Ketones



colloidal SiQD dispersions exhibiting red luminescent upon exposure to a standard hand-held UV light ($\lambda = 365$ nm), consistent with successful surface functionalization.¹⁵ As expected, the colloidal stability of alkoxy-SiQD toluene suspensions improved with increasing alkyl chain length (Figure S1).

FT-IR analyses of SiQDs modified with aliphatic ketones show characteristic spectral features arising from surface bonded alkoxy moieties including: saturated C–H stretching at $2850\text{--}3000\text{ cm}^{-1}$ and C–H bending at 1365 and 1475 cm^{-1} (Figure 1). Absorptions observed at ca. 1100 cm^{-1} can also be attributed to Si–O and C–O stretching, supporting the

presence of the proposed Si–O–R surface-bonding mode. It is important to note that contributions to this absorption arising from surface oxidation cannot be completely ignored.²⁵ Broad absorptions attributed to OSi–H (ca. 2250 cm^{-1}) and Si–H_x (ca. 2100 cm^{-1}) are noted, consistent with incomplete surface coverage similar to that observed for other hydrosilylation products.^{14,36} We also note features related hydrogen-bonded –OH functionalities in some spectra (ca. 3500 cm^{-1}) that may be related to residual solvent (e.g., methanol) and trace surface oxidation.

Additional confirmation of the surface modification of SiQDs via the presented hydrosilylation approach was obtained by evaluating the products obtained from the reactions of acetone-*d*₆ and trifluoroacetone. The FT-IR spectrum of SiQDs modified using acetone-*d*₆ (1f) show a sharp characteristic absorption at 2230 cm^{-1} that is confidently assigned to the C–D stretching mode while those bearing trifluoroacetone-derived surface moieties (1e) show features of C–H stretching and bending, as well as symmetric and asymmetric stretching of C–F bonds at 1200 and 1282 cm^{-1} , respectively (Figure 1b and c).

The presence of surface-bonded alkoxy-moieties was further confirmed using X-ray photoelectron spectroscopy (XPS). The C 1s region of the narrow-scan spectra of all alkoxy-modified materials shows features attributable to the presence of C–C and C–O bonds at 284.8 and 287 eV , respectively (Figure 2, left traces). In all cases, the Si 2p emission of the narrow-scan spectra (Figure 2, right traces) shows an intense feature at 99.3 eV characteristic of core Si atoms (i.e., Si(0)) as well as a high energy shoulder arising from Si-based surface species. Of particular note, fitting the narrow-scan XP spectra of all functionalized samples results in an intense silicon oxide emission centered at 102.3 eV that we tentatively attribute to the Si–OR linkages.²⁸

Proton nuclear magnetic resonance (¹H NMR) spectra (Figure S2), acquired for SiQDs functionalized with longer chain aliphatic ketones (i.e., 2-octanone and 2-dodecanone),³⁷ further confirms functionalization and provides information regarding proton environments within the moieties on the SiQD surfaces. The ¹H NMR spectra of SiQDs functionalized with 2-octanone and 2-dodecanone both show resonances arising from terminal and internal methyl protons at 0.85 and 1.55 ppm , respectively, as well as internal methylene protons in the range of $\sim 1.1\text{--}1.6\text{ ppm}$.

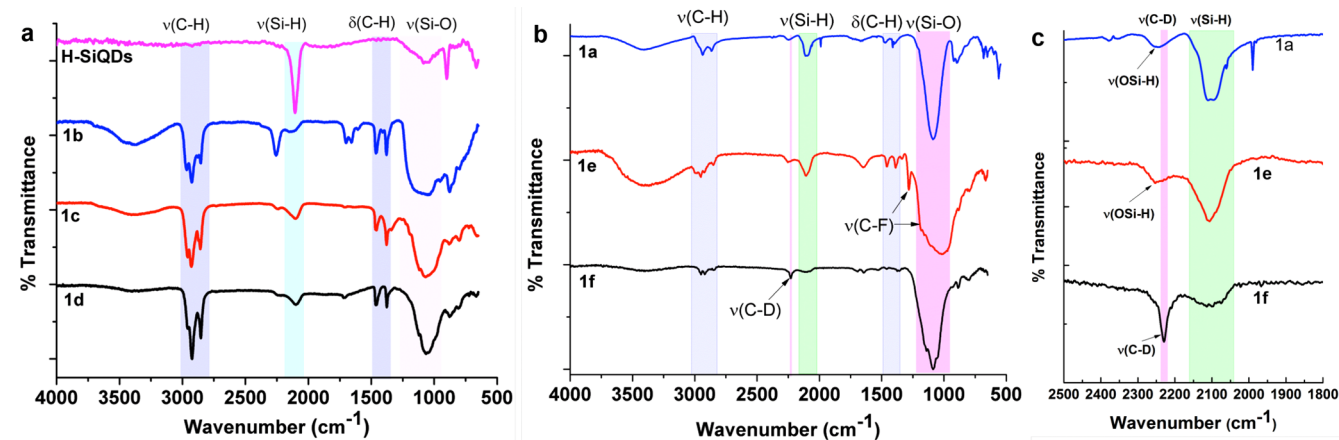


Figure 1. FTIR spectra of alkoxy terminated SiQDs ($d \sim 3$ nm). (a) Hydride terminated SiNCs, and compounds 1b, 1c, and 1d; (b,c) compounds 1a, 1e, and 1f.

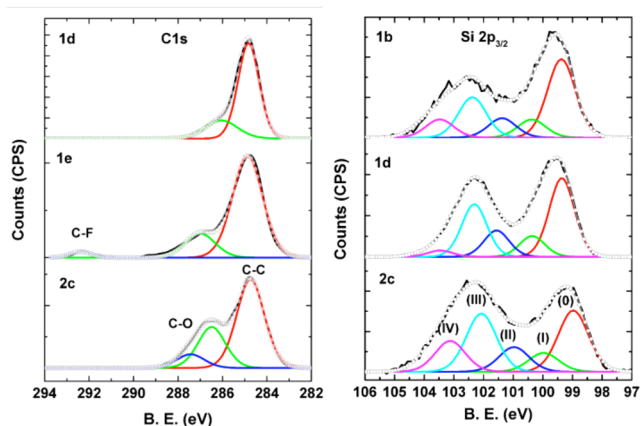


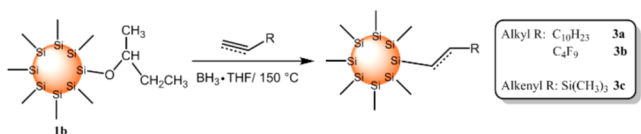
Figure 2. (Left) Narrow-scan XP spectra of C 1s for SiQDs ($d \sim 3$ nm) functionalized with 2-dodecanone (**1d**), trifluoroacetone (**1e**), and dodecanophenone (**2c**). (Right) Narrow-scan XPS of Si 2p region for SiQDs functionalized with 2-butanone (**1b**), 2-dodecanone (**1d**), and dodecanophenone (**2c**). Black curves and circles correspond to the original data and fit spectra, respectively. Fitting results are shown for the Si $2p_{3/2}$ components. The Si $2p_{1/2}$ signals have been omitted for clarity.

In stark contrast to the aliphatic systems noted above, aromatic ketones (e.g., acetophenone, valerophenone, dodecanophenone) undergo hydrosilylation by H-SiQD surfaces at room temperature without the need for any catalyst (Scheme 1b). The FT-IR spectra (Figure S3) of the resulting products show a feature centered at 1600 cm^{-1} that we assign to an aromatic C=C bond and a weak absorption at 3050 cm^{-1} related to aromatic C-H stretching. As is the case with their aliphatic counterparts, Si-O and C-O stretching features are expected to reside under the broad intense feature at ca. 1100 cm^{-1} . Narrow-scan XP spectra of the aromatic products (Figure 2, 2c) show emissions from C-C (284.8 eV) and C-O (286.5 eV) in the C 1s region.

The size and morphology of the functionalized SiQDs were evaluated using TEM and HRTEM. Bright field TEM images (Figure S4) show the functionalized QDs maintain a pseudospherical shape with diameters of $3.4 \pm 0.4\text{ nm}$. Consistent with qualitative observations of SiQD solvent compatibility. HRTEM images of all alkoxy-SiQDs show lattice fringes resulting from Si(111) lattice spacing (d -spacing = 0.32 nm), indicating the Si core remained intact throughout the modification procedure.

Ligand Exchange Reactions on Alkoxy-Terminated SiQDs. At first inspection, one might expect that the strong Si-O linkage (Si-O bond energy = 452 kJ/mol) tethering an alkoxy surface to a SiQD would preclude exchange reactions. However, we have found that the alkoxy-moieties on SiQDs are readily exchanged with alkyl- and alkenyl-functionalities upon heating under microwave irradiation in the presence of a Lewis acid catalyst (Scheme 2). While the presented reaction is

Scheme 2. Preparation of Alkyl/Alkenyl-SiQDs from 2-Butoxy-SiQDs (**1b**) via Ligand Exchange Reactions



effective in modifying SiQDs of varied dimensions (i.e., $d \sim 3, 5, 8\text{ nm}$), for convenience the following discussion will be confined to the representative reactions of 2-butoxy-terminated SiQDs ($d \sim 3\text{ nm}$).

Alkyl- or alkenyl-functionalized SiQDs were obtained via exchange reactions in which 2-butoxy-SiQDs were exposed to an alkene (i.e., 1-dodecene, 1*H*,1*H*,2*H*-perfluoro-1-hexene) or alkyne (i.e., trimethylsilylacetylene; TMSA) of choice in the presence of $\text{BH}_3 \cdot \text{THF}$ in tetrahydrofuran. Ligand exchange reactions involving 1-dodecene and TMSA afforded SiQDs that are compatible with common organic solvents (e.g., toluene) affording transparent suspensions that exhibit orange-red PL upon exposure to a standard hand-held UV light ($\lambda = 365\text{ nm}$). In contrast, perfluoro-hexyl-SiQDs (**3b**) show very limited solubility in organic solvents due to the lipophobic nature of the surface; however, the materials remain photoluminescent.³⁸

The FTIR spectra of SiQDs obtained after ligand exchange show the characteristic features related to the new alkyl/alkenyl groups (Figure 3). The spectrum of 1-dodecyl-terminated

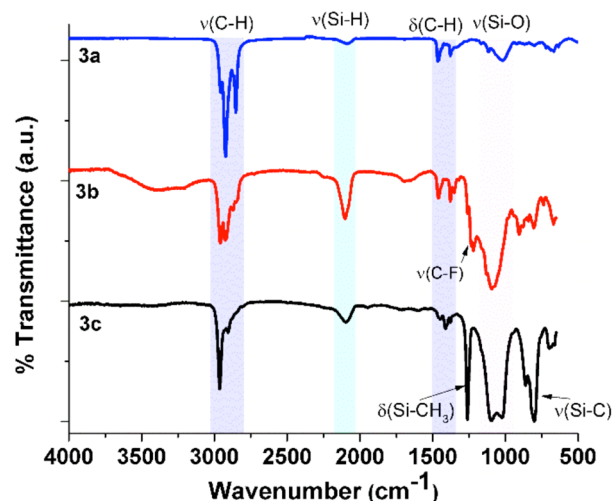


Figure 3. FTIR spectra of dodecyl- (**3a**), perfluorohexyl- (**3b**), and TMSA-SiQDs ($d \sim 3\text{ nm}$) (**3c**) after ligand exchange.

SiQDs is what is expected from previous reports.^{15,16,18} SiQDs terminated with 1*H*,1*H*,2*H*-perfluoro-1-hexyl- moieties (**3b**) display intense symmetric and asymmetric C-F stretching at 1200 and 1282 cm^{-1} , respectively, as well as weak C-H stretching at ca. 2900 cm^{-1} . Similarly, the spectrum of TMSA-functionalized SiQDs (**3c**) shows sharp absorptions at 2900 cm^{-1} (CH_3 stretching), 1260 cm^{-1} (Si- CH_3 umbrella mode), and 800 cm^{-1} (Si-C stretching).

As expected, the Si 2p region of the narrow-scan XP spectra of alkyl/alkenyl-SiQDs (Figure 4) shows an intense emission at 99.3 eV characteristic of core Si atoms as well as high energy emissions arising from Si surface atoms due to Si-C bonds (100.3 eV) and other surface suboxides were observed at 101.3 . Interestingly, the intensity of the feature we attributed to the Si-OR surface species at 102.3 eV is substantially decreased. In addition the C 1s region of the narrow-scan spectrum of dodecyl-SiQDs shows an intense emission at $\sim 285\text{ eV}$ due to C-C/C-H bonds while the same region in the 1*H*,1*H*,2*H*-perfluoro-1-hexyl-SiQDs shows two emissions at 292 and 294 eV arising from the CF_2 and CF_3 , respectively as well as a high energy shoulder on the C-C emission at 284 eV that arises

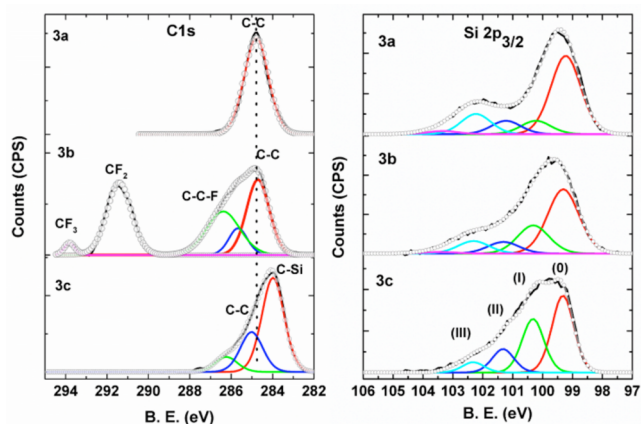


Figure 4. Narrow-scan XPS spectra of C 1s (left) and Si 2p (right) region for dodecyl-SiQDs ($d = 3.4$ nm) (3a), perfluorohexyl-SiQDs (3b), and TMSA-SiQDs ($d \sim 3$ nm) (3c). Black curves and circles correspond to the original data and fit spectra, respectively. Fitting results are shown for the Si 2p_{3/2} components. Si 2p_{1/2} signals have been omitted for clarity.

from C–C–F species.³⁹ As expected, the XP spectrum of TMSA-functionalized SiQDs shows an emission 284 eV.

The ¹H NMR spectra of the present alkyl and alkenyl-functionalized SiQDs show broadened signals related to the target surface species (Figure S5). Specifically, spectra of TMSA-SiQDs show trimethylsilyl-protons with a chemical shift of 0.0 ppm, dodecyl-SiQDs show resonances associated with terminal methyl protons at ~ 0.9 ppm and methylene chain protons in the range of ~ 1.1 to 1.6 ppm; consistent with the expected surface modification, the integration ratio of the methyl to methylene proton signals was 3:20.¹⁶

TEM and HRTEM analyses of the ligand-exchanged SiQDs ($d \sim 3$ nm) bearing dodecyl (3a), 1*H*,1*H*,2*H*-perfluoro-1-hexyl- (3b) and TMSA (3c) confirm the SiQDs retain their pseudospherical morphology and crystalline cores (vide supra). Representative TEM and HRTEM images of three

different sizes of dodecyl-SiQDs obtained from ligand exchange of 2-butoxy-SiQDs were shown in Figure 5. The size distributions of corresponding dodecyl-SiQDs are shown in Figure S6. A comparison of the photoluminescent properties of the present SiQDs (Figure S7) shows that after ligand exchange, products exhibit a slightly red-shifted PL emission maxima compared to the original 2-butoxy-SiQDs (ca. 667 nm). An examination of the radiative lifetime of alkyl- and alkenyl-SiQDs indicates τ has increased from values observed for equivalent 2-butoxy-SiQDs (Table 1). It is reasonable these

Table 1. PL Emission Maxima and Lifetime Decay (τ) of 3 nm SiQDs Functionalized with Various Ketones and Alkenes/Alkynes after Ligand Exchange from 1b

ligands	SiQDs	emission peak maxima	PL lifetime decay (τ)
2-butanone	1b	667 nm	24.4 μ s
2-dodecanone	1d	670 nm	30.2 μ s
dodecanophenone	2c	650 nm	24.5 μ s
1-dodecene	3a	682 nm	40.5 μ s
perfluorohexene	3b	687 nm	39.3 μ s
TMSA	3c	685 nm	45.0 μ s

differences are related surface species on the alkoxy-terminated SiQDs and are the subject of ongoing investigations.⁴⁰ PL emission spectra (Figure S8) of SiQDs (3a) display size dependent PL as the larger QDs after ligand exchange show PL maximum at longer wavelengths: 730 nm (for 5.3 nm) and 928 nm (for 8.2 nm QDs).

Understanding Surface Exchange in SiQDs. Ligand exchange reactions on SiQD surfaces are rare and the presented activation of Si–O bonds on alkoxy-terminated SiQDs is unprecedented. Previously, we reported that BH₃·THF initiated hydrosilylation of alkenes and alkynes proceeds via hydroboration of alkenes/alkynes, followed by transmetalation between hydroboranes and H-terminated SiQDs.¹⁶ Building on our earlier work, we propose that the presented ligand exchange reactions proceed via the mechanism summarized in

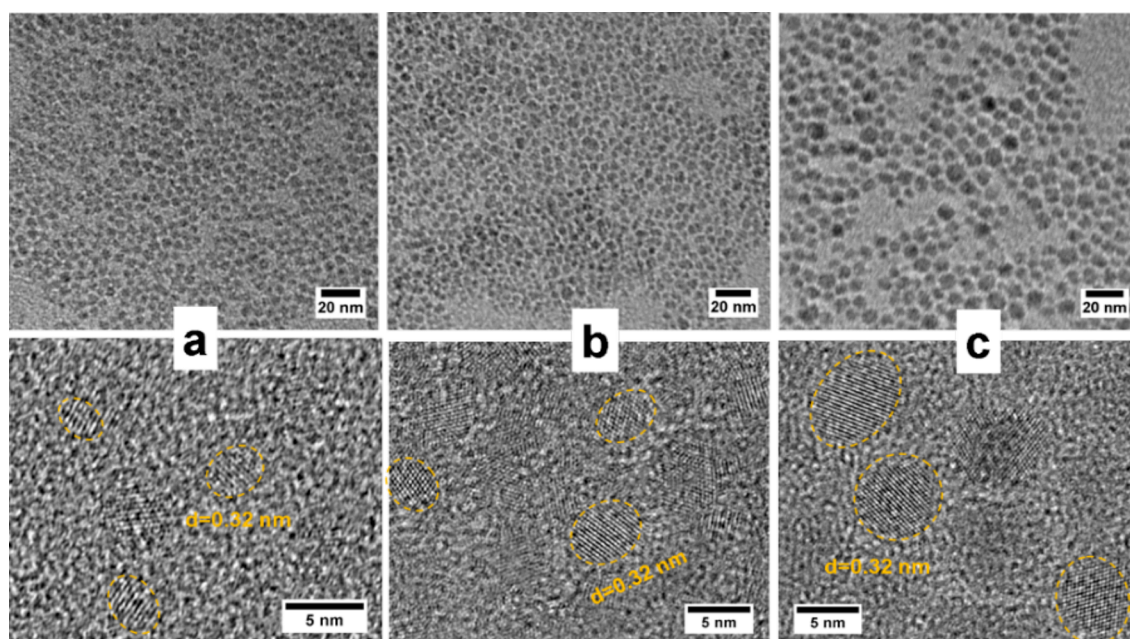
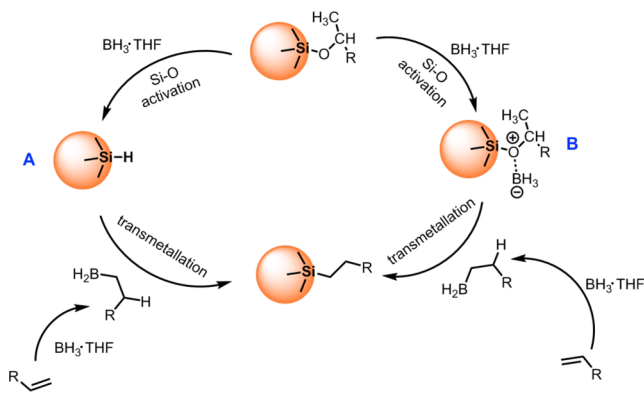


Figure 5. TEM and HRTEM of dodecyl-SiQDs (3a) of (a) 3.4 nm, (b) 5.3 nm, and (c) 8.2 nm obtained from ligand exchange reaction with 1b.

Scheme 3. In the present system, the alkene or alkyne reacts with $\text{BH}_3\cdot\text{THF}$ to form a hydroboration product. Concom-

Scheme 3. Proposed Mechanism of Ligand Exchange Reaction in the Presence of $\text{BH}_3\cdot\text{THF}$



itantly, additional $\text{BH}_3\cdot\text{THF}$ (or B–H of alkyl/alkenyl-borane) activates SiQD surface Si–O bond to form either surface Si–H (path A) or activated complex (path B), followed by transmetalation that produces the Si–C surface linkage. The thermodynamic driving force of this reaction is the breaking of Si–O bonds and forming more stable B–O bonds (e.g., bond energies B–O (536 kJ/mol) > Si–O (452 kJ/mol)).

In support of this proposed mechanism, we performed a model molecular reactions. The first saw tetramethoxysilane (TMOS) being treated with $\text{BH}_3\cdot\text{THF}$ under microwave irradiation at 150 °C and resulted in the production of trimethoxyborane that was confirmed by ^{11}B NMR with chemical shift of 18.5 ppm (Figure S9). The expected silicon-based product (i.e., SiH_4) is a reactive gas and was not detected by NMR.

CONCLUSIONS

In the presented study, the surfaces of H-terminated SiQDs were modified via hydrosilylation of ketones. Aliphatic ketones required exposure to microwave irradiation while aromatic ketones, having a comparatively electron rich carbonyl oxygen, undergo this reaction at room temperature. The resulting alkoxy-terminated SiQD surfaces were air stable and solution processable. Most importantly, they also provide soluble precursors that readily undergo surface exchange reactions and afford the introduction of alkyl/alkenyl-functionality upon exposure to alkenes or alkynes in the presence of $\text{BH}_3\cdot\text{THF}$. This unprecedented reaction, that sees the cleavage of a Si–O linkage, opens the door to straightforward solution phased modification of SiQDs.

MATERIALS AND METHODS

Materials. Hydrogen silsesquioxane (HSQ, trade name Fox-17 was purchased from Dow Corning Corporation (Midland, MI)). Electronic grade hydrofluoric acid (HF, 49% aqueous solution) was purchased from J. T. Baker. $\text{BH}_3\cdot\text{THF}$ (1 M solution in THF), tris(pentafluorophenyl)borane, tetramethoxysilane (TMOS) and chloroform- d_1 (CDCl_3 , 99.9%) were obtained from Sigma-Aldrich and used as received. Acetone, acetone- d_6 , 2-pentanone, 2-octanone, 2-dodecanone, benzaldehyde, valerophenone, 1-dodecene, trimethylsilylacetylene, 1,1,1-trifluoroacetone, and 1H,1H,2H-perfluoro-1-hexene were purchased from Sigma-Aldrich or Alfa Aesar and were purified by passing through activated alumina column and degassed by freeze–pump–thaw cycles before use. Dodecanophenone was purchased from

Sigma-Aldrich and used without further purification. Solvents (e.g., toluene, THF, etc.) were dried using a Grubbs-type solvent purification system¹ manufactured by Innovative Technology, Inc., degassed (freeze–pump–thaw method) and stored under an atmosphere of nitrogen prior to use.

Preparation of H-SiQDs. H-SiQDs were synthesized from HSQ as described previously.^{16,34} Typically, 4 g of HSQ was heated to 1100 °C under reducing gas (5% H_2 / 95% Ar) flow for 1 h and the resulting SiQD/SiO₂ composite was ground mechanically for making 3.4 nm SiQDs. For the present size dependent study, the SiQD/SiO₂ composite was transferred to a carbon boat and annealed at 1200 or 1300 °C for 1 h in Ar atmosphere to prepare 5.3 and 8.2 nm SiQDs, respectively. The dark brown SiQDs/SiO₂ product was ground with agate mortar and pestle for 10–15 min and shaken in a wrist-action shaker overnight with $d \sim 3$ mm borosilicate glass beads. In a PTFE beaker, 500 mg of the resulting composite was dispersed in 10 mL water/ethanol (50%) and etched with 5 mL of 48% HF in the dark for 1 h. (**Caution!** HF is extremely hazardous and must be handled using appropriate protection equipment and procedures.) The H-SiQDs (ca. 40 mg) were isolated from the alcoholic HF mixture upon extraction into toluene (20 mL \times 2) and were isolated by centrifugation at 3000 rpm for 10 min. Nanocrystals were washed twice with 15 mL of toluene and redispersed into 5 mL of dry toluene followed by drying over molecular sieves (4 Å). Finally, the toluene dispersion of H-SiQDs (4 mL) was transferred into a Schlenk flask and degassed by three freeze–pump–thaw cycles on an Ar charged double manifold Schlenk line and used immediately.

Microwave Assisted Hydrosilylation of Aliphatic Ketones. In a typical reaction, 10 mmol of the aliphatic ketone of choice (e.g., 2-butanone) and degassed H-SiQD solution were combined in a 5 mL microwave vial in a N_2 filled glovebox. The microwave vial was sealed and heated to 180 °C using a Biotage initiator microwave chamber for 1h. In all cases a transparent solution was obtained. The reaction mixture containing functionalized SiQDs was concentrated using a rotary evaporator to a final volume of ~ 1 –2 mL. The concentrate was transferred to a 50 mL PTFE centrifuge tube followed by addition of 40 mL of methanol. This procedure yielded a cloudy suspension was centrifuged at 12 000 rpm for 30 min to afford a yellow solid consisting of crude functionalized SiQDs. The pellet was redispersed in toluene and the centrifugation/redispersion procedure was repeated three times to yield purified alkoxy-terminated SiQDs which were dispersed in dry toluene and stored in a screw-capped vial in an ambient atmosphere for further characterization by FTIR, XPS, NMR, and TEM. Only 2-butoxy-SiQDs as representative alkoxy-SiQDs were used for further ligand exchange reaction.

Room Temperature Hydrosilylation of Aromatic Ketones. Dodecanophenone (5 mmol, 1.3 g) was added to 5 mL of degassed toluene suspension of H-SiQD (16 mg) in 50 mL Schlenk flask. The mixture was stirred at room temperature for ~ 12 h under Ar atmosphere after which a transparent orange solution was obtained. The solution was transferred to a 50 mL PTFE centrifuge tube and methanol antisolvent (40 mL) was added to yield a cloudy suspension. After centrifuging at 12 000 rpm for 30 min a yellow pellet containing impure functionalized SiQDs was recovered and the supernatant was discarded. The functionalized SiQDs as a yellow pellet were redispersed in 5 mL toluene and isolated upon addition of 35 mL methanol antisolvent followed by centrifugation at 1200 rpm for 20 min. The redispersion/centrifugation procedure was repeated three times. The final purified aromatic ketone functionalized SiQDs were dispersed in dry toluene and stored in a screw-capped vial in an ambient atmosphere for further characterization.

$\text{BH}_3\cdot\text{THF}$ Mediated Alkoxy-SiQD Ligand Exchange. In a typical reaction 1-dodecene (10 mmol) was added to a solution of 2-butoxy-terminated SiQD (**1b**) (ca. 10 mg SiQDs in 5 mL of dry THF). The reaction mixture was further degassed by three freeze–pump–thaw cycles. The reaction mixture was then cooled to 0 °C in an ice-bath and $\text{BH}_3\cdot\text{THF}$ (10 mmol, 10 mL of 1 M $\text{BH}_3\cdot\text{THF}$ solution in THF) was added through syringe at once. The reaction mixture was stirred for 30 min and then transferred it to microwave vial while maintaining an Ar atmosphere and the microwave vial as sealed. The reaction

mixture was heated in a Biotage initiator microwave chamber at 150 °C for 1 h. The resulting transparent reaction mixture solution was transferred to a 50 mL PFE centrifuge tube and methanol (35 mL) was added to yield a cloudy suspension. Crude surface exchanged SiQDs were isolated as an orange/yellow solid upon centrifuging the mixture at 12 000 rpm for 30 min. The SiQDs were purified upon redispersing in 5 mL toluene and isolated upon addition of 35 mL methanol antisolvent followed by centrifugation. Surface bonded 2-butoxy-motities on SiQDs were exchanged for other alkenes/alkynes using analogous conditions. The purified alkyl/alkenyl-SiQDs were dispersed in dry toluene and stored in a screw-capped vial in an ambient atmosphere for further characterization.

Control Experiment Involving Molecular Alkoxy-Silanes. In a sealed microwave vial, tetramethoxysilane (TMOS, 1 mmol, 152 μ L) and $\text{BH}_3\cdot\text{THF}$ (1.5 mmol, 1.5 mL of 1 M solution in THF) in 3.5 mL of toluene- d_8 were transferred and heated under microwave irradiation at 150 °C for 1 h. The yellow-colored crude reaction mixture was analyzed ^{11}B NMR spectroscopy.

Material Characterization. Fourier transform infrared (FT-IR) spectroscopy was performed using a Thermo Nicolet Magna 750 IR spectrometer. Samples for FT-IR analysis were prepared upon drop coating a toluene solution (ca. 0.25 mL of 1 mg/mL) of the functionalized SiQDs of choice onto an electronic-grade Si-wafer (N-type, 100 surface, 100 mm thickness and 10 ohm-cm resistivity) and dried under air.

Bright field transmission electron microscopy (TEM) images were taken with a JEOL 2011TEM with LaB6 electron gun using accelerating voltage of 200 kV. TEM samples were prepared by depositing a drop of dilute toluene solution (ca. 0.1 mg/mL) of the functionalized SiQD suspensions onto a holey carbon coated copper grid and the solvent was removed in vacuo. The QD size determined upon averaging the dimensions of at least 200 particles using ImageJ software (version 1.45). High resolution (HR) TEM images were obtained using a Hitachi-9500 electron microscope with an accelerating voltage of 300 kV. The HRTEM images were processed using Gatan Digital Micrograph software (version 2.02.800.0).

Photoluminescence (PL) spectra of functionalized SiQDs in cyclohexane (spectroscopic grade) were acquired using a Cary Eclipse spectrophotometer ($\lambda_{\text{ex}} = 350$ nm) or by illuminating the cuvette with a 445 nm diode laser and monitoring the emission using an Ocean Optics USB2000 spectrometer calibrated using a Micropack HL-2000-FHSA blackbody source. PL lifetimes were acquired upon illuminating a quartz cuvette containing solution samples using a modulated argon ion laser (476 nm, ~ 30 mW). The laser was modulated by an acousto-optic modulator operating at 500 Hz. Emission from the SiQDs was channeled into a photomultiplier (Hamamatsu H7422P-50) connected to a photon counting card (PMS-400A). Lifetime decay data was fit to a stretched exponential function in Mathematica (version 10) given by

$$I(t) = I_0[\exp(-(t/\tau)^\beta)] + C$$

where I_0 is the initial photon intensity, τ is the effective lifetime, and β is a stretching parameter that can vary between 0 and 1 (smaller values indicate broader lifetime distributions).⁴¹

Proton nuclear magnetic resonance (^1H NMR), and $^{11}\text{B}\{^1\text{H}\}$ NMR spectra were acquired for samples dissolved in CDCl_3 using Varian Unity Inova Console 500 MHz NMR spectrometer. The fid files were processed in Nuts Pro software.

X-ray photoelectron spectroscopy (XPS) analyses were performed using a Kratos Axis Ultra instrument operating in energy spectrum mode at 210 W. Samples were prepared by drop coating a solution of functionalized SiQDs (ca. 0.25 mL of 2 mg/mL) onto a copper foil substrate to yield thin films. The base and operating chamber pressure were maintained at 10^{-7} Pa. A monochromatic Al $K\alpha$ source ($\lambda = 8.34$ Å) was used to irradiate the samples, and the spectra were obtained with an electron takeoff angle of 90°. To minimize sample charging, the charge neutralizer filament was used when required. Survey spectra were collected using an elliptical spot with major and minor axis lengths of 2 and 1 mm, respectively, and 160 eV pass energy with a step of 0.33 eV. CasaXPS software (VAMAS) was used to interpret

high-resolution spectra. All spectra were internally calibrated to the C 1s emission (284.8 eV). After calibration, a Shirley-type background was applied to remove most of the extrinsic loss structure. The fwhm for all the fitted peaks was maintained below 1.2 eV.

■ ASSOCIATED CONTENT

📄 Supporting Information

The Supporting Information is available free of charge on the ACS Publications website at DOI: 10.1021/jacs.6b03155.

FTIR, NMR, PL spectra, TEM, size distribution, and additional supporting figures (PDF)

■ AUTHOR INFORMATION

Corresponding Authors

*jveinot@ualberta.ca

*purkait@ualberta.ca

Present Address

†M.I.: McKetta Dept of Chemical Engineering, University of Texas at Austin, Texas 78712, United States.

Notes

The authors declare no competing financial interest.

■ ACKNOWLEDGMENTS

The Veinot team recognizes the Natural Science and Engineering Research Council of Canada (NSERC) Discovery Grant Program for continued generous financial support as well as financial contributions from the ATUMS training program supported by NSERC CREATE Program. We would also like to acknowledge Prof. Al Meldrum, Kai Cui, and the staff at Nanofab for assistance with material characterization. Dr. John Washington and all Veinot group members are also thanked for useful discussion.

■ REFERENCES

- (1) Ding, Y.; Dong, Y.; Bapat, A.; Nowak, J. D.; Carter, C. B.; Kortshagen, U. R.; Campbell, S. A. *IEEE Trans. Electron Devices* **2006**, *53*, 2525–2531.
- (2) Walters, R. J.; Bourianoff, G. I.; Atwater, H. A. *Nat. Mater.* **2005**, *4*, 143–146.
- (3) Priolo, F.; Gregorkiewicz, T.; Galli, M.; Krauss, T. F. *Nat. Nanotechnol.* **2014**, *9*, 19–32.
- (4) Perez-Wurfl, I.; Hao, X.; Gentle, A.; Kim, D.-H.; Conibeer, G.; Green, M. A. *Appl. Phys. Lett.* **2009**, *95*, 153506.
- (5) Islam, M. A.; Purkait, T. K.; Veinot, J. G. C. *J. Am. Chem. Soc.* **2014**, *136*, 15130–15133.
- (6) Dasog, M.; Kehrle, J.; Rieger, B.; Veinot, J. G. C. *Angew. Chem., Int. Ed.* **2016**, *55*, 2322–2339.
- (7) Veinot, J. G. C. *Chem. Commun.* **2006**, 4160–4168.
- (8) Dasog, M.; De los Reyes, G. B.; Titova, L. V.; Hegmann, F. A.; Veinot, J. G. C. *ACS Nano* **2014**, *8*, 9636–9648.
- (9) Bhattacharjee, S.; Rietjens, I. M. C. M.; Singh, M. P.; Atkins, T. M.; Purkait, T. K.; Xu, Z.; Regli, S.; Shukaliak, A.; Clark, R. J.; Mitchell, B. S.; Alink, G. M.; Marcelis, A. T. M.; Fink, M. J.; Veinot, J. G. C.; Kauzlarich, S. M.; Zuilhof, H. *Nanoscale* **2013**, *5*, 4870–4883.
- (10) Park, J.-H.; Gu, L.; von Maltzahn, G.; Ruoslahti, E.; Bhatia, S. N.; Sailor, M. J. *Nat. Mater.* **2009**, *8*, 331–336.
- (11) Regli, S.; Kelly, J. A.; Barnes, M. A.; Andrei, C. M.; Veinot, J. G. C. *Mater. Lett.* **2014**, *115*, 21.
- (12) Warner, J. H.; Hoshino, A.; Yamamoto, K.; Tilley, R. D. *Angew. Chem., Int. Ed.* **2005**, *44*, 4550–4554.
- (13) Linford, M. R.; Fenter, P.; Eisenberger, P. M.; Chidsey, C. E. D. *J. Am. Chem. Soc.* **1995**, *117*, 3145–3155.
- (14) Hua, F.; Swihart, M. T.; Ruckenstein, E. *Langmuir* **2005**, *21*, 6054–6062.

- (15) Yang, Z.; Gonzalez, C. M.; Purkait, T. K.; Iqbal, M.; Meldrum, A.; Veinot, J. G. C. *Langmuir* **2015**, *31*, 10540–10548.
- (16) Purkait, T. K.; Iqbal, M.; Wahl, M. H.; Gottschling, K.; Gonzalez, C. M.; Islam, M. A.; Veinot, J. G. C. *J. Am. Chem. Soc.* **2014**, *136*, 17914–17917.
- (17) Kelly, J. A.; Shukaliak, A. M.; Fleischauer, M. D.; Veinot, J. G. C. *J. Am. Chem. Soc.* **2011**, *133*, 9564–9571.
- (18) Yang, Z.; Iqbal, M.; Dobbie, A. R.; Veinot, J. G. C. *J. Am. Chem. Soc.* **2013**, *135*, 17595–17601.
- (19) Kelly, J. A.; Veinot, J. G. C. *ACS Nano* **2010**, *4*, 4645–4656.
- (20) Holland, J. M.; Stewart, M. P.; Allen, M. J.; Buriak, J. M. *J. Solid State Chem.* **1999**, *147*, 251–258.
- (21) Kovalenko, M. V.; Manna, L.; Cabot, A.; Hens, Z.; Talapin, D. V.; Kagan, C. R.; Klimov, V. I.; Rogach, A. L.; Reiss, P.; Milliron, D. J.; Guyot-Sionnest, P.; Konstantatos, G.; Parak, W. J.; Hyeon, T.; Korgel, B. A.; Murray, C. B.; Heiss, W. *ACS Nano* **2015**, *9*, 1012–1057.
- (22) Yu, Y.; Rowland, C.; Schaller, R. D.; Korgel, B. A. *Langmuir* **2015**, *31*, 6886–6893.
- (23) Tian, F.; Teplyakov, A. V. *Langmuir* **2013**, *29*, 13–28.
- (24) Zou, J.; Baldwin, R. K.; Pettigrew, K. A.; Kauzlarich, S. M. *Nano Lett.* **2004**, *4*, 1181–1186.
- (25) Bell, J. P.; Cloud, J. E.; Cheng, J.; Ngo, C.; Kodambaka, S.; Sellinger, A.; Ratanathanawongs Williams, S. K.; Yang, Y. *RSC Adv.* **2014**, *4*, 51105–51110.
- (26) Lee, P. T. K.; Skjel, M. K.; Rosenberg, L. *Organometallics* **2013**, *32*, 1575–1578.
- (27) Boukherroub, R.; Morin, S.; Sharpe, P.; Wayner, D. D. M.; Allongue, P. *Langmuir* **2000**, *16*, 7429–7434.
- (28) Khung, Y. L.; Ngalim, S. H.; Meda, L.; Narducci, D. *Chem. - Eur. J.* **2014**, *20*, 15151–15158.
- (29) Khung, Y. L.; Ngalim, S. H.; Scaccabarozzi, A.; Narducci, D. *Sci. Rep.* **2015**, *5*, 11299.
- (30) Hacker, C. A.; Anderson, K. A.; Richter, L. J.; Richter, C. A. *Langmuir* **2005**, *21*, 882–889.
- (31) Hong, Q.; Rogero, C.; Lakey, J. H.; Connolly, B. A.; Houlton, A.; Horrocks, B. R. *Analyst* **2009**, *134*, 593–601.
- (32) Parks, D. J.; Piers, W. E. *J. Am. Chem. Soc.* **1996**, *118*, 9440–9441.
- (33) Rendler, S.; Oestreich, M. *Angew. Chem., Int. Ed.* **2008**, *47*, 5997–6000.
- (34) Hessel, C. M.; Henderson, E. J.; Veinot, J. G. C. *Chem. Mater.* **2006**, *18*, 6139–6146.
- (35) The average diameters of the SiQDs were evaluated after the functionalization of H-SiQDs with various ketones and the later by ligand exchange reactions.
- (36) Jariwala, B. N.; Dewey, O. S.; Stradins, P.; Ciobanu, C. V.; Agarwal, S. *ACS Appl. Mater. Interfaces* **2011**, *3*, 3033–3041.
- (37) The shorter chain systems were not investigated by NMR because because of solubility limitation.
- (38) Qian, C.; Sun, W.; Wang, L.; Chen, C.; Liao, K.; Wang, W.; Jia, J.; Hatton, B. D.; Casillas, G.; Kurylowicz, M.; Yip, C. M.; Mastronardi, M. L.; Ozin, G. A. *J. Am. Chem. Soc.* **2014**, *136*, 15849–15852.
- (39) Pujari, S. P.; Spruijt, E.; Cohen Stuart, M. A.; van Rijn, C. J. M.; Paulusse, J. M. J.; Zuillhof, H. *Langmuir* **2012**, *28*, 17690–17700.
- (40) Yang, Z.; De los Reyes, G. B.; Titova, L. V.; Sychugov, I.; Dasog, M.; Linnros, J.; Hegmann, F. A.; Veinot, J. G. C. *ACS Photonics* **2015**, *2*, 595–605.
- (41) Berberan-Santos, M. N.; Bodunov, E. N.; Valeur, B. *Chem. Phys.* **2005**, *315*, 171–182.